A Cellular Model for Spatial Population Dynamics

Chu Yue (Stella) Dong[a], James T. Long[b], Clifford A. Reiter[c], Corey Staten[d], Rytis Umbrasas[e]
a – 2080 1st Ave. Apt. 1809, New York, NY 10029, USA
b – 809 Montbard Drive, West Chester, PA 19382, USA
c – Department of Mathematics, Lafayette College, Easton, PA 18042-1781, USA
d – 528 Hilltonia Ave, Columbus, OH 43223, USA
e – Lafayette College, P.O. Box 9486, Easton, PA 18042, USA

Abstract

Interacting populations exhibit complex behavior in nature. Classic quadratic iteration models with two or three populations exhibit some of the features seen in nature, but fail to account for spatial variation. Indeed, the diversity paradox is that many classic population models predict one species dominates while nature exhibits diversity. While various schemes have been presented to address this dilemma, we present a simple, deterministic cellular model that incorporates classic iteration schemes and a spatial migration component that provides for self-organizing and rich behavior. Our visualization method allows us to observe dynamically changing predominance of species, global diversity, waves of species progression, and highly organized spiral structures.

Keywords: cellular automata, population cycles, continuous automata, predator-prey

1. Introduction

The population levels of species in some ecosystems may fluctuate over time in fairly regular intervals. Classic illustrations of this phenomenon can be seen in fur records collected by the Hudson's Bay Company Northern Department. Figure 1 shows lynx population data from [1] with muskrat population data from [2] from 1821 to 1891. Note that there is an approximate cycle of ten years and that peaks of the lynx population roughly correspond to troughs of the muskrat population. This observation provides motivation for studying predator-prey differential or difference equations since they can exhibit linked oscillating populations [3-5]. However, they do not exhibit the diversity in time and space observed in nature. Ecologists are well aware of the diversity paradox and that spatial variation [6-9] and disturbances [10] play an important role in population dynamics.

Cellular models classically consist of a regular, discrete arrangement of cells taking values from a finite set with states updated simultaneously at discrete time steps according to a local rule [11,12]. The local rule is the same for each cell and only depends upon the state of neighbors in some predefined finite neighborhood. In this paper, we use a square lattice of cells with states being lists of the population levels of the multiple species being modeled. Thus, unlike traditional cellular automata, we allow each cell to contain a collection of continuous states from the real numbers (representing population levels). The local rule we present is completely deterministic. It uses a mixing scheme that allows us to simulate migration patterns for each species and iteration of a classic system of nonlinear difference equations at each cell. The iteration scheme allows for the detrimental or beneficial aspect of interactions of populations to be expressed. While the local rule we investigate is unique, the model has similarities to coupled map lattices and is in the spirit of many reaction-diffusion models that have been extensively studied [6,7,11,12]. A cellular model is also used in [6] but the iteration scheme is different from what we examine.

We thus investigate a multispecies population model that accounts for both interspecies and spatial interactions. Our visualization scheme allows for multiple population levels to be simultaneously viewed throughout the area used for the simulation. We will see that rich behavior may arise, population levels may oscillate, waves of predominant species may sweep across the landscape, succession of species may be observed, and in certain situations, highly organized spirals may develop from random configurations.

2. Classic cellular models exhibiting rich behavior

Before presenting our population model, we consider two known examples of cellular models that exhibit self-organizing behavior. We do this in order to have examples of complex behavior that utilize simple, but different modeling strategies. First is a discrete probabilistic cellular automaton known as the WATOR model [11]. Each cell in the lattice represents a single fish, shark, or an empty cell (i.e. water). Fish swim at random to an adjacent unoccupied cell and breed one of their kind after a specified number of generations. Sharks also swim at random to an adjacent cell that is either unoccupied or occupied by a fish. Each shark breeds one of its kind after a certain number of generations. Sharks also have to eat fish in order to survive; if a shark does not eat any fish in a specified number of generations, it will die. The behavior of the model depends on four parameter values, but with suitable choice of parameters and initial conditions, an increase in the number of fish leads to an increase in the number of sharks and the increase in the number of sharks leads to the decrease in the number of fish, thus achieving global balance but local diversity. Figure 2 shows an image from a simulation of WATOR with random initial conditions. The model exhibits self-organizing behavior, but it is agent based and uses random choices in the update process.

The second example is the hodgepodge machine. It is a deterministic continuous cellular automaton in which each cell in the lattice can be healthy (value 0), infected (value between 0 and 1) or ill (value 1). Each healthy cell becomes infected if a threshold of infection among neighbors is exceeded and each ill cell becomes healthy at the next time step. Infected cells have a tendency to increase their level of infection at each time step. Figure 3 shows an example after 200 steps of the hodgepodge machine applied to a random initial configuration from [13]; notice that the hodgepodge machine self-organized into dramatic spirals. Details of the update rule and parameters may also be found in [13].

Like WATOR, the model we present in the next section allows there to be patches of changing dominant population. However, our model is deterministic. Like the hodgepodge machine, it can also produce self organization. However, since our scheme is multi-species, it can exhibit succession of species. It can also produce stability and extinction.

3. Population dynamics with spatial mixing for two species

In the multispecies population model we are presenting, each cell represents the population levels of predator(s), prey or resource(s). These will be updated according to pre-defined local rules. For simplicity, we first describe our model in the case where there are two populations. Let $x = x_{I,J}$ denote the level of the prey population in cell (*I*, *J*) and $y = y_{I,J}$ the level of the predator population in cell (*I*, *J*). Our local update rule consists of two stages. First, each of the population levels is averaged in a weighted manner over the immediate 3 by 3 neighborhood around the cell. This provides for migration or diffusion of populations. We let m_x and m_y denote migration coefficients for *x* and *y*. We compute the local average *x* value for each cell by taking m_x times the average over the 3 by 3 neighborhood plus $1-m_x$ times the center cell. We do likewise for the other populations. Specifically, in the first phase we compute the following.

$$\begin{aligned} \overline{x}_{I,J} &= (1-m_x)x_{I,J} + \frac{1}{9}m_x \sum_{i,j\in\{-1,0,1\}} x_{I+i,J+j} \\ \overline{y}_{I,J} &= (1-m_y)y_{I,J} + \frac{1}{9}m_y \sum_{i,j\in\{-1,0,1\}} y_{I+i,J+j} \end{aligned} \tag{1}$$

The second phase is motivated by the difference equations of Lotka-Volterra type [3-5,7] that can then be used to describe the interspecies interactions. For example, the changes in population levels in a predator-prey model have the following form where *A* is a growth rate for the prey, *B* gives a prey-prey competition factor, *C* determines the rate at which the prey is diminished by interactions, *D* is a growth (death) rate for the predator, *E* is the rate at which the predator is increased by prey-predator interactions, and *F* is a predator-predator competition term.

$$\begin{aligned} \Delta x &= x^{new} - x = Ax - Bx^2 - Cxy \\ \Delta y &= y^{new} - y = -Dy + Exy - Fy^2 \end{aligned} \tag{2}$$

The classic Lotka-Volterra model is a differential equation analogue of (2) with *B* = *F* = 0. Classic competition models are similar with different choices of sign.

The second phase of our local scheme is to update the averaged populations in each according to (2). In particular, solving for x^{new} and y^{new} in (2) and replacing *x* and *y* by the averages from (1), our assembled local rule is:

$$\begin{aligned} x^{new}_{I,J} &= (A+1)\overline{x}_{I,J} - B\overline{x}^{\,2}_{I,J} - C\overline{x}_{I,J}\,\overline{y}_{I,J} \\ y^{new}_{I,J} &= (1-D)\overline{y}_{I,J} + E\,\overline{x}_{I,J}\,\overline{y}_{I,J} - F\,\overline{y}^{\,2}_{I,J} \end{aligned} \tag{3}$$

Our convention is to list the parameters in an array with minus signs explicit and the first column corresponding to the linear terms. That is, we would write

$$\begin{pmatrix} A+1 & -B & -C \\ 1-D & E & -F \end{pmatrix} \tag{4}$$

for the above. Figure 4 shows a typical example of a two species system run on a 200 by 200 arrangement of cells with periodic boundary conditions. Here the intensity of red at a position indicates the level of the first (prey) population while the intensity of green shows the level of the second (predator) population. Parameters for this system are

$$\begin{pmatrix} 1.5 & -0.00002 & -0.001 \\ 0.5 & 0.0001 & -0.00001 \end{pmatrix} \tag{5}$$

where $m_x = m_y = 1$. Initial conditions were a random distribution as will be explained in the next section. After 100 steps the two populations have formed distinct patches. By step 200 the populations have organized so that there are distinct waves of predators moving into regions of high prey concentration. Figure 5 shows the behavior of the two populations in a single cell over the 200 steps. The population levels oscillate with the same period but out of phase in a manner reminiscent of Figure 1. Like natural populations, the height of the peaks tends to vary. An animation of this cellular model with these parameters may be found at [14].

4. Fixed points and stability

In general we consider models with *n* species. Each cell contains *n* population levels $x_1, x_2, \ldots, x_n$ with local averaging and an update rule for x_i involving a linear term for x_i and quadratic terms that are x_i times each of the population levels.

$$x_i^{new} = x_i\left(1 + a_{i,0} + \sum_{j=1}^{n} a_{i,j} x_j\right), \qquad i = 1,2,\ldots,n. \tag{6}$$

We can analyze this quadratic iteration scheme as a discrete nonlinear dynamical system. Considering and interpreting fixed points and eigenvalues is a standard technique [4,5,7,15]. Of course, in our model the mixing plays a significant role. Nonetheless, we can understand some behaviors of the iteration scheme mathematically and use that for guidance. The fixed points of the system are the points where $x_i^{new} = x_i$. Thus, the nonzero fixed points of (6) will correspond to solutions to the following linear system.

$$a_{i,0} + \sum_{j=1}^{n} a_{i,j} x_j = 0, \qquad i = 1,2,\ldots,n. \tag{7}$$

For typical choices of $a_{i,j}$ the system will have a unique nonzero fixed point. The fixed point offers some guidance that can be used for selecting the visualization scale or the initial configuration. For example, our typical random configuration selects each population uniformly between zero and twice the level of that population at the fixed point.

Moreover, if the right hand side of (6) is viewed as a vector valued function of the vector of population levels, the Jacobian can be computed. The Jacobian is the matrix giving the partial derivatives of all the right hand sides with respect to all the variables. The eigenvalues of the Jacobian evaluated at the fixed point give an indication of the qualitative behavior that might be expected for a pure iteration scheme near the fixed point. For example, if we look at the data for the example shown in Figure 4, the fixed point is approximately (5392, 3922). The eigenvalues are a complex conjugate pair with magnitude approximately 1.03. Thus we would expect the iteration scheme to involve a rotation and slight expansion near the fixed point. Figure 6 shows the succession of (*x*,*y*) pairs for one cell from the model. The cell begins by moving in toward the fixed point and next rotates around it in an expanding fashion. We will see that the migration scheme has a great impact on the overall behavior, but we can still use an understanding of the iteration scheme to get a sense of scale and to select examples where the eigenvalues of the Jacobian of the fixed point would seem to be interesting. In particular, when complex pairs are near one in magnitude or when some eigenvalues are smaller than one while others are larger would be a good place to look for rich behavior.

Combining the migration phase with the iteration leads to the following general form for our *n*-species model. Here we use $x_{i,I,J}$ to denote the level of the *i*th population in cell (I,J).

$$\bar{x}_{i,I,J} = \left(1 - m_{x_i}\right)x_{i,I,J} + \frac{1}{9} m_{x_i} \sum_{i,j\in\{-1,0,1\}} x_{i,I+i,J+j}$$

$$x_{i,I,J}^{new} = \bar{x}_{i,I,J}\left(1 + a_{i,0} + \sum_{j=1}^{n} a_{i,j} \bar{x}_{j,I,J}\right), \qquad i = 1,2,\ldots,n. \tag{8}$$

Similar to (1), $\overline{x}_{i,I,J}$ is a weighted average over the immediate 3 by 3 neighborhood using the migration coefficient m_{x_i}.

5. Population dynamics with spatial mixing for three species

More complex behavior is observed in three species systems. Figure 7 shows the behavior after 65 and 200 steps for a system with random initial conditions. It shows very typical spiral wave formation. Here the three population levels correspond to the intensity of red, green and blue. After 65 iterations patches have formed while after 200 spiral wave fronts appear. An animation for this example, a script to run the process, and the coefficients may be found at [14]. Here the populations might be interpreted as resource, prey and predator and the wave fronts have a distinct predator follows prey follows resource ordering.

Other choices of parameters and migration schemes may lead to visually uninteresting behaviors. The populations may all settle down on the fixed point. Sometimes one population becomes extinct and the others behave like one with fewer species.

Figures 8-9 both correspond to the exact same coefficients; however, the migration rates differ. Figure 8 has migration rates $< 0.5, 1, 0.1 >$ while Figure 9 has $< 1, 0.5, 1 >$. Note that in Figure 7 distinct patches appear, but there is only a hint of spirals. The spirals in Figure 9 are distinct. Compare these with those from the hodgepodge machine as seen in Figure 3.

In our implementation we also forced population levels to be between zero and some convenient upper bound. The upper bound played no role in the examples discussed so far, but in the next two examples they do play a role. Figures 10 and 11 arise from the same coefficient matrix and a random initial condition that is sparse for the second two populations. In Figure 10 the model is bounded by 2^{16}-1 and in practice the first two populations periodically reach the bound while the third never reaches it. In Figure 11 the model is bounded by 2^{24}-1 and in practice the first two populations do not reach the bound but, curiously, the third population does periodically reach the bound. The behavior appears less organized and is qualitatively different from that seen with the lower bound.

6. Conclusions

A deterministic cellular multispecies population model that iterates the process of migration between cells and updating cells according to a quadratic iteration scheme is presented. It gives rise to rich self-organizing behavior. We visualize the population levels using different color components so that we can observe the interaction of the populations including global diversity, and recycling waves of species progression as might be expected in nature. We see single cells exhibit out of phase periodic behavior like seen in nature. We also see dramatic, self organized spirals appear from random.

Acknowledgements

This work was supported by NSF grant DMS-055282 and Lafayette College’s EXCEL program.

References

[1] Elton C, Nicholson M. The ten-year cycle in numbers of the lynx in Canada. The Journal of Animal Ecology 1942;11(2):215-244.

[2] Elton C, Nicholson, M. Fluctuations in numbers of the muskrat (Ondatra Zibethica) in Canada. The Journal of Animal Ecology 1942;11(1):96-126.
[3] Giordano FR, Weir MD, Fox WP. A first course in mathematical modeling, Pacific Grove: Brooks Cole; 2003.
[4] May RM. Stability and complexity in model ecosystems: Princeton University Press; 1973.
[5] Tilman D, Kareiva P, ed. Spatial ecology, the role of space in population dynamics and interspecies interactions: Princeton University Press; 1997.
[6] Bjornstad ON, Bacompte J. Synchrony and second order spatial correlation in host-parasitoid hierarchies. Journal of Animal Ecology 2001; 70 (6) 924-933.
[7] Cantrell RS, Cosner C. Spatial ecology via reaction-diffusion equations: John Wiley & Sons; 2003.
[8] Jongejans E, Skarpaas O, Shea K. Dispersal, demography and spatial population models for conservations and control management. Perspectives in Plant Ecology, Evolution, and Systematics 2008;9:153-170.
[9] Smith CH. Spatial trends in Canadian Snowshoe Hare, Lepus americanus, population cycles. Canadian Field-Naturalist 1983;97(2):151-160.
[10] Pascual M, Guichard F. Criticality and disturbance in spatial ecological systems. Trends in Ecology and Evolution; 20 (2) 88-95.
[11] Schiff JL. Cellular automata: a discrete view of the world. Hoboken: John Wiley & Sons, Inc; 2008.
[12] Wolfram S. A new kind of science, Champaign: Wolfram Media; 2002.
[13] Reiter CA. Fractals, visualization, and J. 3rd ed. Lulu; 2007.
[14] Dong CY, Long JT, Reiter CA, Staten C, Umbrasas R, A cellular model for spatial population dynamics auxiliary materials. http://www.lafayette.edu/~reiterc/mvq/cmspd/index.html 2008.
[15] Martelli M. Discrete dynamical systems: John Wiley & Sons, Inc; 1992.

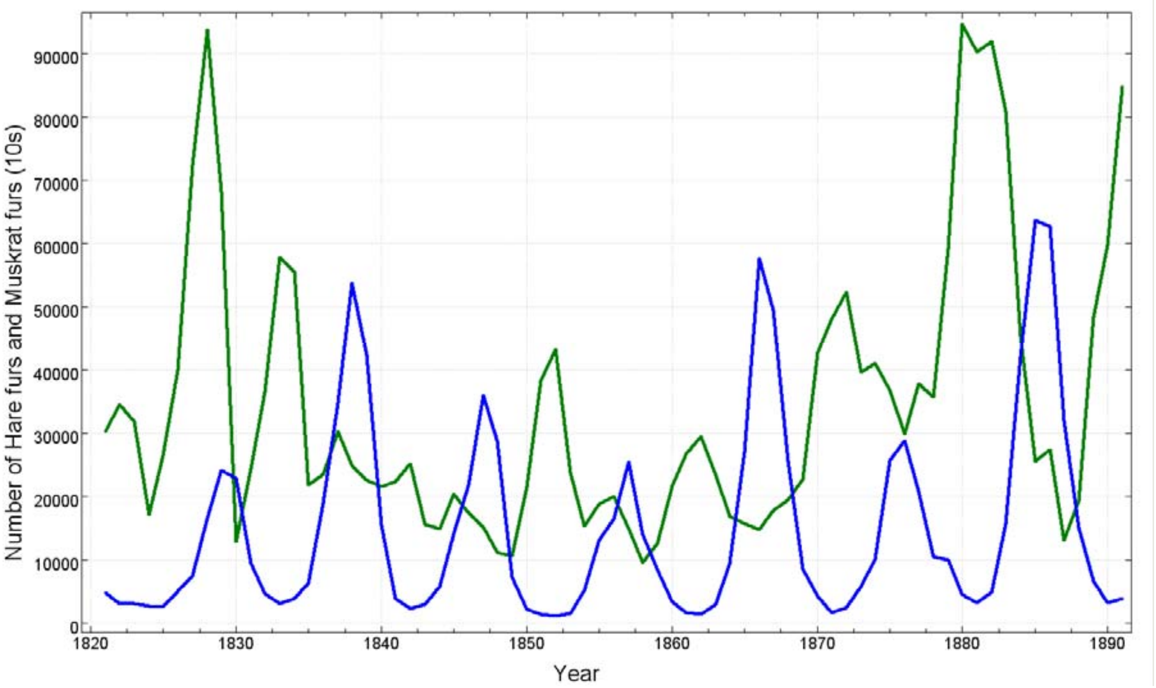

Figure 1. Lynx furs (blue) and muskrat furs (green, 10s) from the Canadian Northern Department of the Hudson's Bay Company.

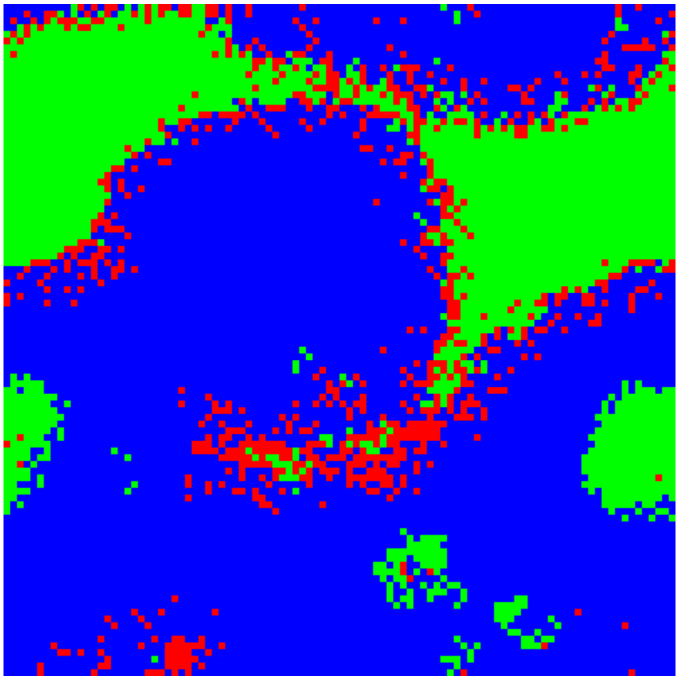

Figure 2. WATOR model of water-fish-sharks.

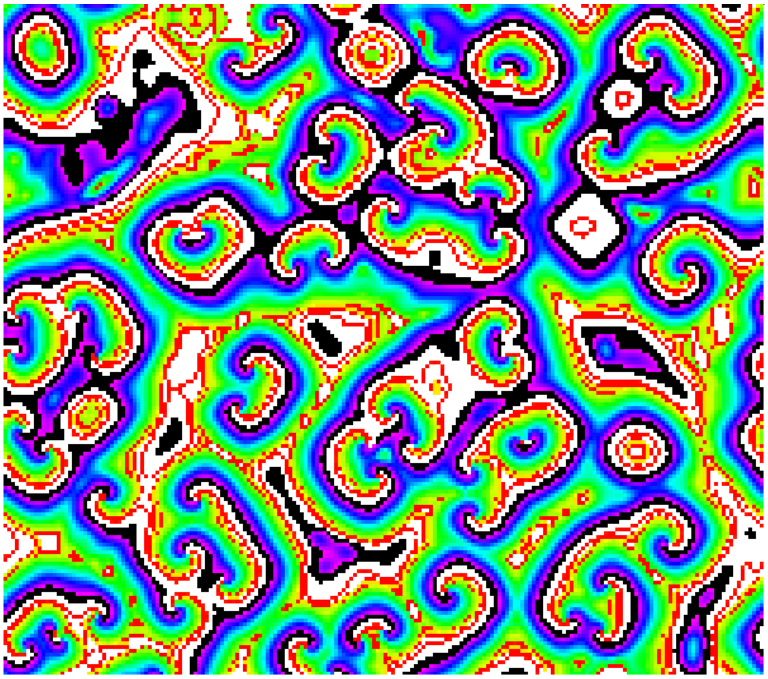

Figure 3. The hodgepodge machine can exhibit self-organizing spirals.

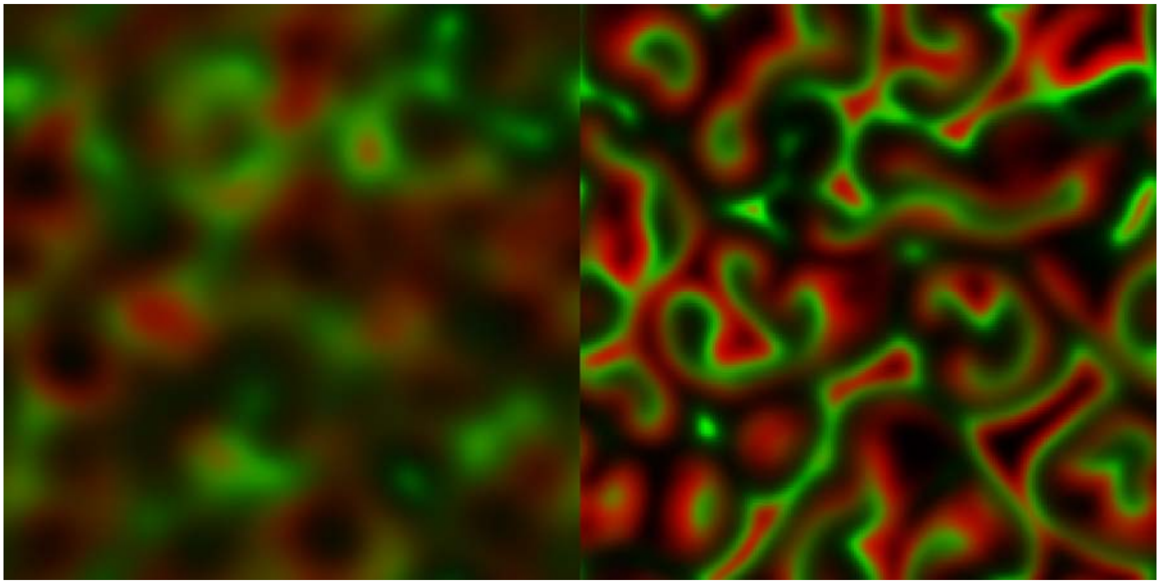

Figure 4. Levels of two populations at time 100 and 200 show predator front formation.

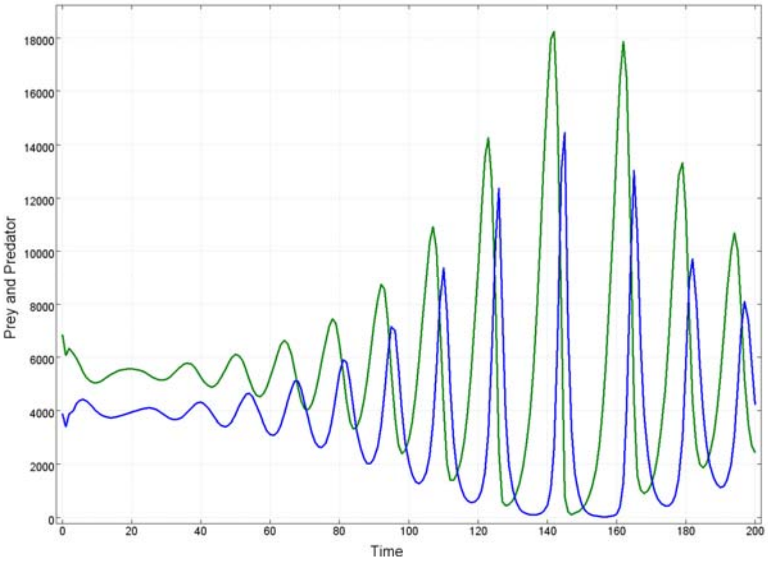

Figure 5. Cyclic variations of the predator and prey population levels at a typical cell.

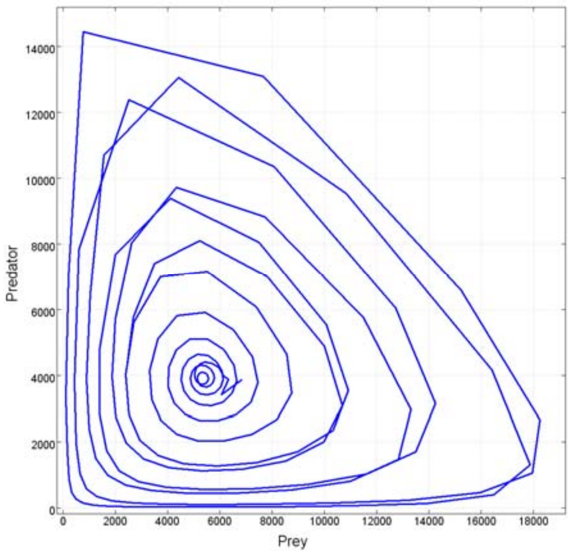

Figure 6. Phase portrait for the predator and prey population levels at a typical cell.

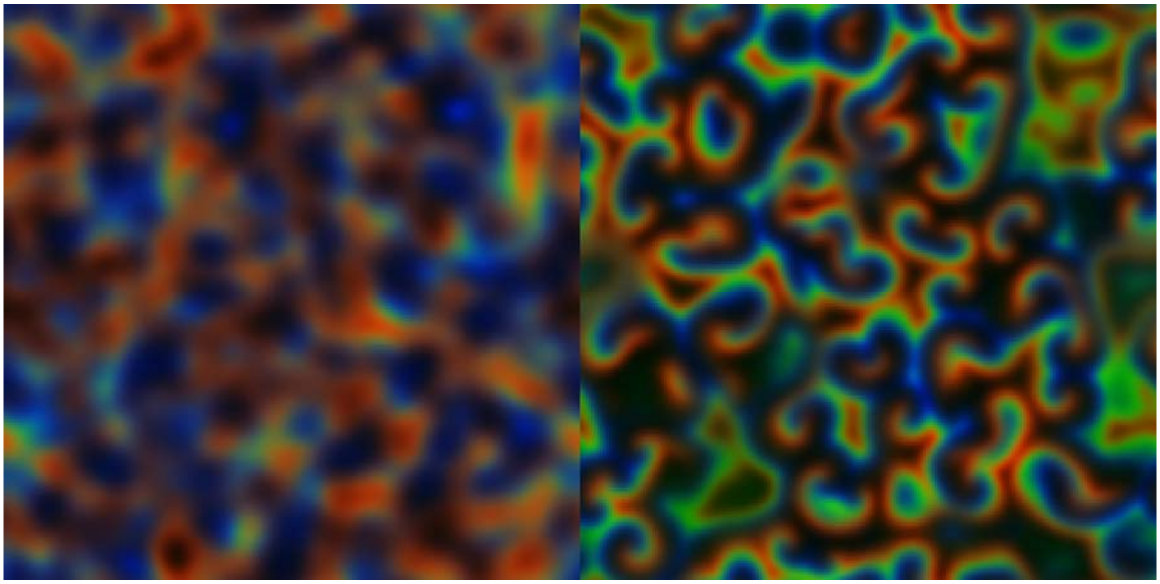

Figure 7. A three-species example at time 65 and 200.

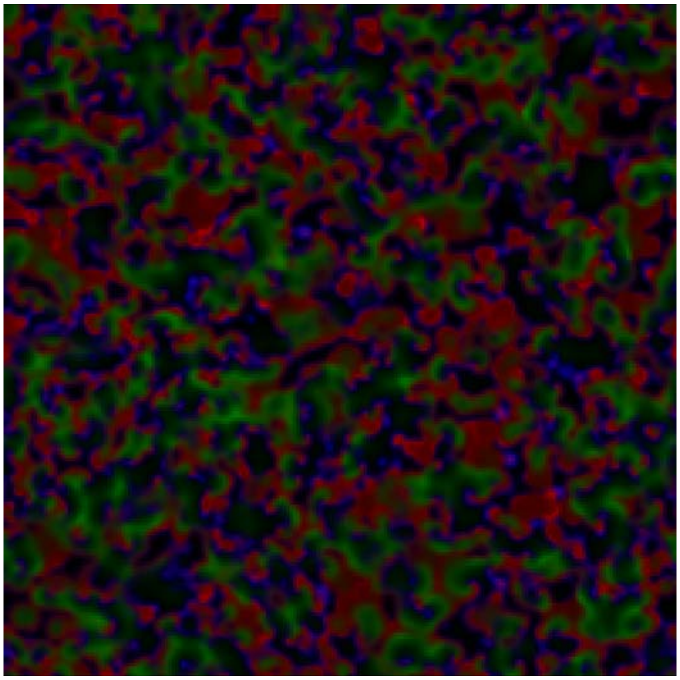

Figure 8. Light formation of spirals for one set of migration values.

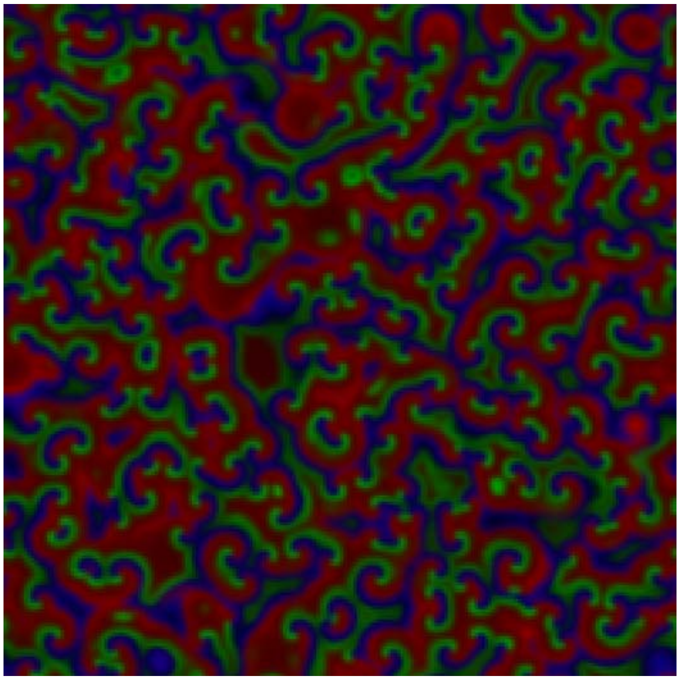

Figure 9. Well formed spirals for another set of migration values.

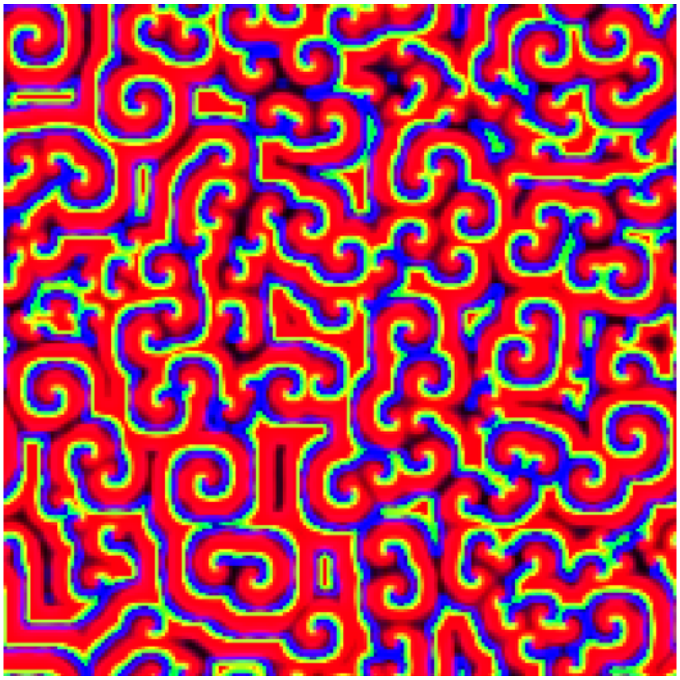

Figure 10. Very distinct spirals for one choice of upper bound.

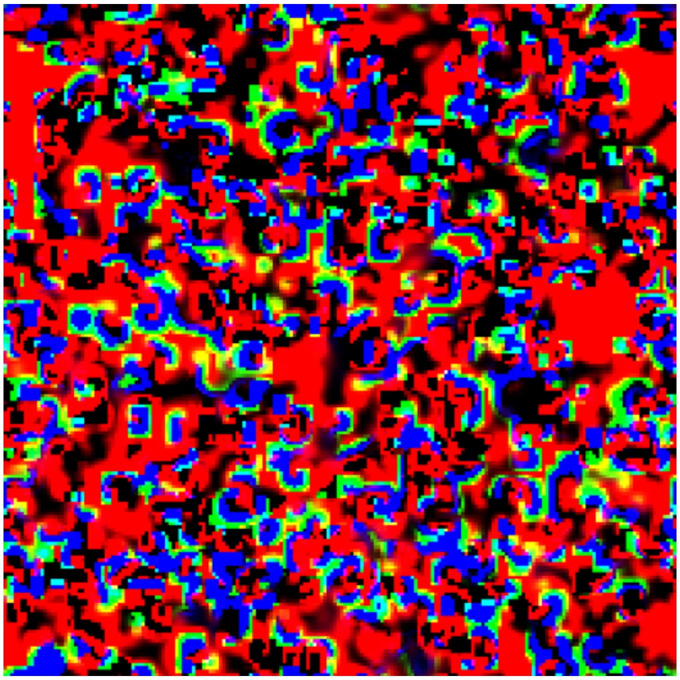

Figure 11. Less organized behavior for a higher upper bound.